NANO LETTERS

Letter

pubs.acs.org/NanoLett

Photothermal Self-Oscillation and Laser Cooling of Graphene Optomechanical Systems

Robert A. Barton,[†] Isaac R. Storch,[‡] Vivekananda P. Adiga,[†] Reyu Sakakibara,[⊥] Benjamin R. Cipriany,[†] B. Ilic,[∥] Si Ping Wang,[‡] Peijie Ong,[§] Paul L. McEuen,[‡,#] Jeevak M. Parpia,[‡] and Harold G. Craighead*[,†]

[†]School of Applied and Engineering Physics, [‡]Department of Physics, and [§]Department of Materials Science and Engineering, Cornell University, Ithaca, New York 14853, United States

[⊥]Department of Chemistry, University of California, Berkeley, Berkeley, California 94720, United States

[∥]Cornell NanoScale Science and Technology Facility, Cornell University, Ithaca, New York 14853, United States

[#]Kavli Institute at Cornell for Nanoscale Science, Cornell University, Ithaca, New York 14853, United States

Supporting Information

ABSTRACT: By virtue of their low mass and stiffness, atomically thin mechanical resonators are attractive candidates for use in optomechanics. Here, we demonstrate photothermal back-action in a graphene mechanical resonator comprising one end of a Fabry−Perot cavity. As a demonstration of the utility of this effect, we show that a continuous wave laser can be used to cool a graphene vibrational mode or to power a graphene-based tunable frequency oscillator. Owing to graphene's high thermal conductivity and optical absorption, photothermal optomechanics is efficient in graphene and could ultimately enable laser cooling to the quantum ground state or applications such as photonic signal processing.

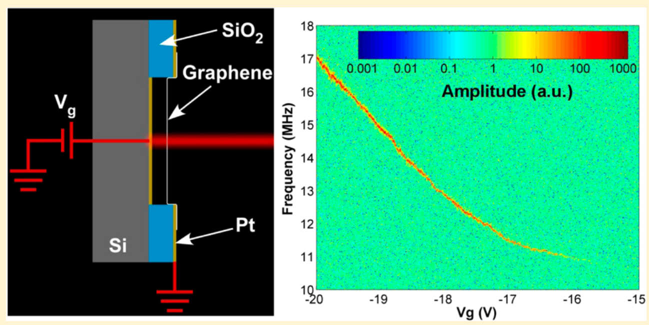

KEYWORDS: *Graphene, optomechanics, nanoelectromechanical systems (NEMS), photothermal force, laser cooling, self-oscillation*

Optomechanics,[1,2] which uses optical feedback and other "back-action" forces to control mechanical elements, has generated much interest since it was applied to micro- and nanomechanical systems.[3] Research in optomechanics has largely focused on using back-action to cool mechanical modes of mesoscopic resonators toward their quantum ground state, with progress first shown using photothermal forces in metal-coated cantilevers[4] and later demonstrated using radiation pressure forces on mirrors,[5−7] membranes,[8] and strings.[9] Many other potential applications for optomechanics have also emerged, such as force sensing,[10] nonvolatile mechanical memory,[11] and photonic signal processing.[12,13] For all of these applications, it is desirable to have a mechanical resonator with low mass and therefore low stiffness $K = m\omega^2$ in order to improve the sensitivity of the structure to the forces of light. There are additional benefits associated with low stiffness, e.g., it allows for cavity tuning of optical resonance for filters, and it increases the amplitude of zero-point motion $x_{zp}^2 = \hbar\omega/2K$. As a result, the drive to reduce the size of the mechanical elements has been an important enabling factor for recent milestones, such as optical cooling of a resonator to the quantum ground state.[14] Ideally, the mechanical element would be reduced to the limit of atomic thickness, but such a resonator would need to have both good mechanical properties and strong coupling to light, which is challenging for such a small object.

Graphene, a single layer of carbon atoms in a hexagonal lattice, is uniquely poised to meet these challenges. Mechanical resonators made from graphene[15−18] are simple to fabricate,[19] benefit from graphene's high strength and Young's modulus,[20] and have demonstrated frequencies as high as 178 MHz,[21] with quality factors of up to 2400 at room temperature[22] and 100 000 at 100 mK.[23] In addition, graphene's optoelectronic properties ensure a strong ($\pi\alpha = 2.3\%$), constant absorption of light across a wide range of wavelengths.[24] Studying optomechanical coupling resulting from this absorption could shed light on photothermal processes in graphene,[25] with applications in, e.g., bolometry.[26] Optomechanical back-action cooling of graphene could also be useful, since the relatively high zero-point motion and frequency of graphene resonators make them ideal candidates[27] for mechanical systems in the quantum regime.[14,28,29] Despite graphene's advantages, no mechanism for optomechanical back-action coupling to these membranes has yet been demonstrated.

We investigated the optomechanical behavior of a graphene resonator forming one end of a low-finesse Fabry−Perot cavity. We found strong photothermal coupling between the light and the graphene, leading to optical back-action that can be used to

Received: May 29, 2012
Revised: August 1, 2012
Published: August 13, 2012

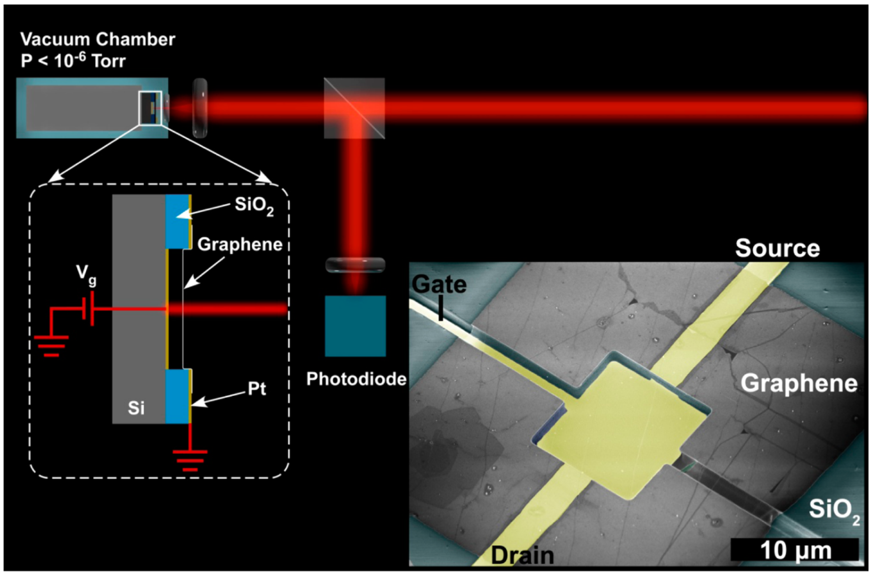

Figure 1. Experimental setup. A laser at either visible or IR wavelengths reflects from the cavity formed between the graphene and the platinum backplane; variations in the reflected laser light are monitored by a photodiode. A gate voltage V_g is applied between the graphene and the underlying electrode; this voltage is sometimes modulated for measurements of driven motion. Inset: a false-color SEM of a typical graphene membrane resonator.

cool the graphene (i.e., reduce its thermal motion) or to counter the mechanical damping of a resonant mode, inducing self-oscillation. Our graphene optomechanical resonators have fundamental flexural mode effective masses as small as $m_{\mathrm{eff}} \approx$ 100 fg, comparable to that of the smallest optomechanical systems demonstrated to date[30] and nearly 2 orders of magnitude lower than that of other electrically integrated optomechanical systems.[31] In contrast with other systems that have demonstrated similar photothermal effects,[3,4,32,33] graphene's low stiffness in combination with strong electrostatic coupling enables tuning of the resonant frequency by more than 100% over 15 V.[17] Strong electrostatic mechanical frequency tunability is a novel feature for optomechanical systems and will be useful for applications in signal processing, while the low stiffness of graphene at relatively high frequencies makes graphene optomechanical systems relevant for the pursuit of mechanical systems in the quantum regime.

The resonators used for this experiment are suspended single-layer graphene clamped on all sides to a silicon dioxide substrate with source, drain, and gate electrodes (Figure 1). The resonators were batch-fabricated from chemical vapor deposited (CVD) graphene[19] following procedures detailed in the Supporting Information. The gap between the graphene and the metal gate acts as an optical cavity from which the reflectivity R is dependent on the displacement z of the graphene toward the backplane. To monitor mechanical resonance, a continuous wave (CW) laser impinges on the cavity, and reflected laser light is modulated by an amount proportional to $z(\omega)\cdot dR/dz$.[34] The reflected light is monitored by a fast photodiode connected to a network analyzer. Motion is actuated capacitively by applying a modulated voltage V_g between the graphene and the gate. The graphene device is placed inside of a vacuum chamber in which the pressure is less than 10^{-6} Torr. We present results for two devices, a suspended square of graphene ("Device 1") and a suspended circle of graphene ("Device 2") (see Supporting Information).

We characterize the resonators by driving their motion capacitively and optically monitoring their response at low laser powers, where optomechanical effects are minimized. Amplitude of motion as a function of frequency and gate voltage for Device 1 is shown in Figure 2a. Previous work[17,18] has shown that the shape of the frequency as a function of gate voltage can be used to extract the density of the resonator. For Device 1, the areal density is $\rho = 5 \times \rho_{\mathrm{graphene}}$, corresponding to a total device mass of m = 700 fg ($m_{\mathrm{eff}} \approx$ 200 fg assuming that the contaminating mass[17,22] is evenly distributed). For Device 2, the same calculation gives $\rho = 3 \times \rho_{\mathrm{graphene}}$ and m = 200 fg ($m_{\mathrm{eff}} \approx$ 100 fg). At a given gate voltage, amplitude versus frequency curves (Figure 2b) fit well to a Lorentzian, allowing us to extract the fundamental frequency ω_0, the full width at half-maximum power (fwhm) Γ, and the quality factor $Q = \omega_0/\Gamma$.

As CW laser intensity is increased, we find that the damping as measured by the fwhm depends on laser power. For laser wavelength λ = 568 nm, the effective damping Γ_{eff} increases linearly with power (Figure 2d), whereas at λ = 633 nm, Γ_{eff} decreases linearly with power (Figure 2e). The dependence of the effect on both power and wavelength demonstrates that the damping is the result of an interaction with the optical cavity. According to the theory for optomechanical coupling to a low-finesse cavity, if there is a light-induced force F on the membrane that acts with time delay τ, such as radiation pressure or a photothermal force, the effective damping Γ_{eff} should follow[35]

$$\Gamma_{\mathrm{eff}} = \Gamma\left(1 + Q\frac{\omega_0\tau}{1 + {\omega_0}^2\tau^2}\frac{\nabla F}{K}\right) \tag{1}$$

where $\nabla F = dF/dz$. The difference in the sign of the optomechanically induced damping $\Gamma_{\mathrm{OM}} \equiv \Gamma Q(\omega_0\tau/(1 + {\omega_0}^2\tau^2))(\nabla F/K)$ between λ = 568 and 633 nm is consistent with an effect in which the force is proportional to the optical energy flux absorbed by the graphene $W_a(z)$; calculations (Figure 2c) show that dW_a/dz has a different sign for λ = 633 and 568 nm. The frequency shifts over the same range are dominated by the static change in membrane tension from laser heating (see Supporting Information).

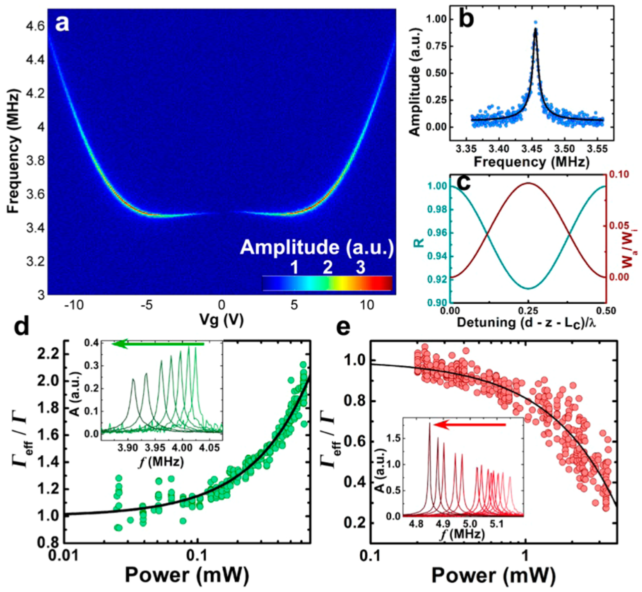

Figure 2. (a) Amplitude of the reflected light as a function of frequency and gate voltage for Device 1 at low laser power (300 μW). (b) Amplitude as a function of frequency at $V_g = 5$ V from (a) is fit to a Lorentzian, yielding $\omega_0 = 2\pi \times 3.46$ MHz, $\Gamma = 2\pi \times 6800$ Hz, and $Q = 500$. (c) Calculated cavity reflectivity R and graphene absorbed energy flux W_a normalized by the incident energy flux W_i as a function of detuning from the resonant cavity length L_c. For the cavity length of Device 1, $(d - L_c)/\lambda = 0.45$ for $\lambda = 568$ nm and $(d - L_c)/\lambda = 0.10$ for $\lambda = 633$ nm; the change in sign of dW_a/dz leads to opposite optomechanical damping in (d,e). (d) Damping increases as a function of CW laser power ($\lambda = 568$ nm) for capacitively driven graphene resonance. (e) Damping decreases with CW laser power ($\lambda = 633$ nm) for capacitively driven graphene resonance. For (d,e), the data are plotted on a semilogarithmic scale to clearly show a broad range of powers; black lines are fits to a linear dependence of Γ_{eff}/Γ on power. Insets show amplitude versus frequency plots; red and green arrows represent increasing powers.

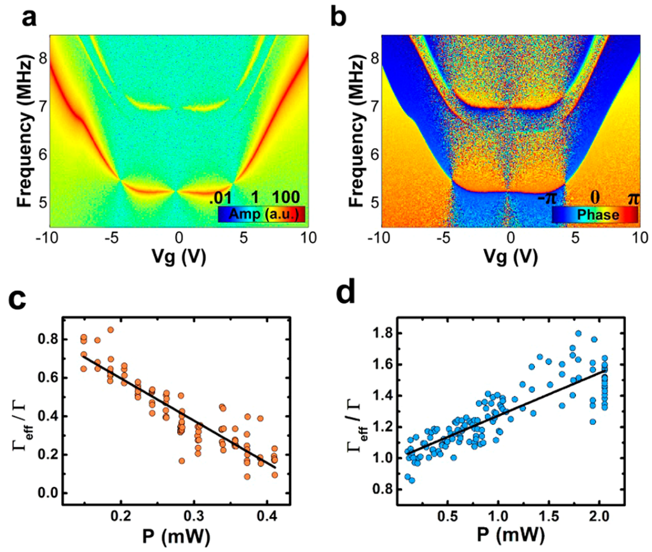

Figure 3. (a) Log-scale amplitude as a function of frequency $\omega/2\pi$ and V_g for Device 2 ($\lambda = 532$ nm, $P = 500$ μW). (b) The phase of the signal relative to the electrical drive as a function of frequency and V_g. The phase shift noticeable as a change in color at a given frequency at ± 4.3 V indicates that dR/dz has changed sign. The sign of dW_a/dz changes simultaneously. (c) Measurements at $V_g = -10$ V show that damping decreases with laser power (Γ_{OM} is negative). (d) Measurements at $V_g = 2$ V show that damping increases with laser power (Γ_{OM} is positive).

The electrostatic gate voltage can be used to tune the optical properties of the cavity, as shown in Figure 3 for Device 2. In Figure 3a, the mechanical resonant frequency is usually visible as it tunes with gate voltage. However, at $V_g \approx \pm 4.3$ V, the signal vanishes because the membrane is at a maximum of reflectance where dR/dz changes sign. Because dR/dz and dW_a/dz change sign simultaneously (Figure 2c), we expect that the sign of Γ_{OM} should also differ depending on whether $|V_g| < 4.3$ V. Indeed, we find that at $V_g = -10$ V, Γ_{OM} is negative (Figure 3c), while at $V_g = 2$ V, Γ_{OM} is positive (Figure 3d). Therefore, at a fixed wavelength $\lambda = 532$ nm, the sign of the optomechanical damping can be controlled by electrical cavity detuning.

The observed optomechanical effects can be understood using a two-dimensional model for a circular drumhead resonator. The feedback observed here requires that the motion of the membrane induce a force that acts on the resonator parallel to the velocity and with some time delay. Candidates include photothermal forces and radiation pressure. First, we calculate how such a force could arise from photothermal effects, i.e., changes in tension of the membrane due to laser-induced heating. In order to explain how tension could provide a force in the z-direction, we consider the case in which the center of the membrane is displaced by an initial amount z_0, leading to a contact angle θ_0 between the plane of the chip and the membrane.[33] Such a displacement must arise, e.g., from a dc gate voltage. In this case, a component of the photothermal force acts along the direction of motion z (see Supporting Information), causing a photon-induced rigidity

$$\nabla F_{pth} = AP\frac{4\pi^2 a}{\lambda}\sin(\theta_0)\sin\left(\frac{4\pi}{\lambda}(d - z_0)\right) \tag{2}$$

where a is the radius of the membrane, λ is the laser wavelength, P is the incident laser power, and d is the distance of the membrane from the gate in the absence of gate voltage. The proportionality constant A indicates how much the tension in the membrane changes with incident laser power. We obtain A empirically by using the frequency shift with increased laser power near $V_g = 0$ as a measure of laser-induced stress; we find $A = 15$ N/(m·W), in reasonable agreement with the value expected from thermal expansion. Estimating τ and θ_0, we find that the predictions of eqs 1 and 2 agree to within approximately an order of magnitude with the results observed in Figure 3c,d. We also consider the possibility of an optomechanical effect from radiation pressure, but the force is too weak to affect either the frequency or the damping of the graphene resonators. Additionally, we study the dependence of Γ_{OM} on both λ and V_g and find that it agrees with eq 2. Thus, we conclude that the optomechanical back-action is caused by photothermal forces (see Supporting Information).

When the damping from the light field Γ_{OM} is negative, sufficiently high laser powers will cause regenerative self-oscillation in the graphene membrane.[3,36] Figure 4a shows the amplitude of oscillation of Device 1 as a function of CW laser power with a dc gate voltage $V_g = -12$ V applied. No time-varying drive force is applied to the graphene. At low laser powers, the graphene vibrates due to Brownian motion. As laser power is increased, the amplitude of motion increases rapidly, demonstrating regenerative self-oscillation. Like the driven oscillation, the self-oscillation of the membrane can be tuned in

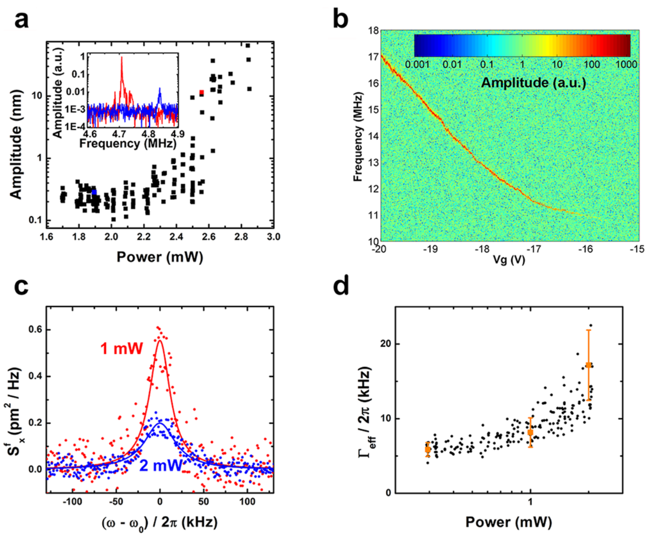

Figure 4. Optomechanically induced self-oscillation and cooling for Device 2 (b only) and Device 1 (all other figures). Data in (a−c) were acquired by applying only a continuous wave laser and a dc gate voltage to the devices. (a) Amplitude of oscillation as a function of CW laser power, with $V_g = -12$ V, $\lambda = 633$ nm. The reflectance amplitude is calibrated to displacement using the thermal motion at low powers.[15] Inset: Examples of log-scale amplitude of oscillation versus frequency for two different laser powers: 1.9 mW (blue) and 2.6 mW (red). The dramatic increase in amplitude for the small increase in laser power is evidence of self-oscillation. (b) Log-scale amplitude versus frequency and gate voltage at $\lambda = 532$ nm, $P = 1.5$ mW, showing that the frequency can be tuned as the device is self-oscillating. (c) Laser cooling of a graphene membrane at $\lambda = 718$ nm. Brownian noise spectra shown for laser powers of 1 mW (red) and 2 mW (blue) are calibrated using the method from ref 15. At the higher laser power, the area under the curve diminishes by a factor of 2, demonstrating that the membrane has been cooled. (d) Width of the driven peak versus laser power at $\lambda = 718$ nm (black); measurements at specific powers (orange) are used to estimate the effective temperature of the undriven peaks in (c).

frequency. Figure 4b shows the self-oscillation of Device 2, which can be tuned in frequency from 11 to 17 MHz as gate voltage is changed from $V_g = -16$ to -20 V. Tunable-frequency self-oscillation of a graphene membrane is useful for applications in photonics and signal processing.[12] In Figure 4b, the graphene acts as a frequency-tunable modulator of light requiring only a gate voltage to adjust its resonant frequency. Of further interest is injection locking behavior,[37] demonstrated here using both electrical and optical pilot signals (see Supporting Information). This behavior could be used to synchronize two optomechanical resonators via electrical or optical signals or for optomechanical amplification.

When Γ_{OM} is positive, the laser can be used to cool the thermal motion of the membrane. At $\lambda = 718$ nm, the area under the Device 1 Brownian motion peak decreases by about a factor of 2 when laser power increases from 1 to 2 mW (Figure 4c). We calculate the effective temperature T_{eff} by noting that the width of the driven motion is also inversely proportional to temperature:[35]

$$\frac{T_{eff}}{T} = \frac{\Gamma}{\Gamma_{eff}} \tag{3}$$

where T and Γ are the temperature and damping at low laser power, respectively. The width Γ_{eff} of the driven motion as a function of power is shown in Figure 4d. According to eq 3, the temperature at $P = 1$ mW is 210 ± 60 K, and the temperature at $P = 2$ mW is 100 ± 40 K. These temperatures are consistent with the change in area under the Brownian motion peaks. We note that the laser-induced heating of the graphene at $P = 2$ mW is less than $\Delta T \approx 20$ K at maximum possible absorption (see Figure 2c and Supporting Information).

We consider the possibility of using graphene optomechanical resonators for room temperature applications in force and position sensing. The ability to resolve the thermal motion of graphene indicates a position sensitivity of 600 fm/Hz$^{1/2}$ for the membrane laser-cooled to 100 K. This sensitivity is limited by noise from the photodetector and corresponds to a force sensitivity of 300 aN/Hz$^{1/2}$, comparable to that of state-of-the-art silicon cantilevers at room temperature[38] but achieved using significantly smaller device dimensions. It could be further improved by cryogenic cooling and taking advantage of optomechanical effects[39] or by incorporating the graphene membrane into a high-finesse cavity.[8]

We also consider the application of graphene resonators to future experiments in quantum mechanics. First, we evaluate the minimum possible temperature that can be reached with laser cooling via the photothermal effect:[35]

$$\frac{T_{eff,min}}{T} = \frac{1}{1 + Q/2} \tag{4}$$

which yields $T_{eff,min} = 1$ K when applied to Device 1 at $T = 293$ K. This is not sufficient to reach the quantum ground state of the resonator at $T_Q = \hbar\omega/k_B = 0.2$ mK from room temperature. However, the graphene resonator studied in ref 19 has a resonant frequency of 75 MHz and $Q = 9000$ at 9 K, from which optomechanical cooling to the quantum ground state is possible according to eq 4. Although there is no fundamental limitation that would prevent cooling to the ground state by a photothermal effect,[40,41] it is challenging because the cooling effect must be strong enough to compensate for heating due to absorbed laser power. We analyze these competing effects in the Supporting Information and conclude that the strength of the cooling effect observed here is large enough to cool the aforementioned 75 MHz resonator from 9K to the quantum ground state, assuming it could be engineered such that $\omega_0\tau = 1$. This result is attributable to the fact that the observed photothermal effect is relatively large despite the low cavity finesse. In Figure 3c we estimate $\nabla F \approx 0.01$ N/m at 500 μW, compared to $\nabla F \approx 0.001$ N/m at 130 μW in ref 4. We note that the optomechanical effect observed here is different in two major ways from previously observed bimetallic expansion effects in metal-coated cantilevers.[4] First, fully clamped graphene membranes can utilize their intrinsic tension for optomechanical feedback, whereas cantilevers have no such tension. Second, graphene has unusually high thermal conductivity,[42] which here enables feedback at nanosecond time scales and could allow scaling of graphene optomechanics into the GHz regime.

We have demonstrated photothermal back-action coupling to a graphene membrane, with potential applications in photonic signal processing and quantum electromechanical systems. The ultimate limits of laser cooling by this technique require testing at low base temperatures, where the quality factor will improve and the thermal transport properties of graphene will differ. It is also important to note that for other areas of optomechanics that can benefit from low-mass membranes, such as coupling to clouds of laser-cooled atoms,[43] radiation pressure coupling would be ideal. For this reason, investigation of alternate means of optomechanical coupling to graphene and other two-dimensional materials is needed. However, as a means of achieving optomechanical coupling to graphene, the technique described here has the advantage that the devices are simple to fabricate and the effect is powerful without a high-finesse cavity, obviating the need for further engineering. Compared to other materials that have been used for photothermal optomechanics, graphene resonators offer the advantages of strong mechanical frequency tunability and an extremely low mass that enhances their frequency-to-stiffness ratio. In general, graphene optomechanical systems provide a way to strongly couple mechanical, optical, and electrical degrees of freedom within a single material, which will enable experimentation in mechanical nonlinear dynamics.

■ ASSOCIATED CONTENT

Ⓢ Supporting Information

Further theoretical and experimental details demonstrating that the optomechanical effect is generated by photothermal forces. Description of devices and fabrication. Injection locking behavior of graphene optomechanical systems and limits of photothermal cooling. This material is available free of charge via the Internet at http://pubs.acs.org.

■ AUTHOR INFORMATION

Corresponding Author

*E-mail: hgc1@cornell.edu

Notes

The authors declare no competing financial interest.

■ ACKNOWLEDGMENTS

We acknowledge discussions with Meredith Metzler, Kathryn McGill, Natalia Shabaltas, Arend van der Zande, Yoav Linzon, Juraj Topolancik, Eric Smith, Sunil Bhave, and Kevek Innovations. Fabrication was performed at the Cornell NanoScale Facility, a member of the National Nanotechnology Infrastructure Network, which is supported by the National Science Foundation (grant ECS-0335765). This work was supported by the Cornell Center for Materials Research (CCMR) with funding from the Materials Research Science and Engineering Center Program of the National Science Foundation (cooperative agreement DMR 0520404 and 0908634), the MARCO Focused Research Center on Materials, Structures, and Devices, and the AFOSR MURI.

■ REFERENCES

(1) Kippenberg, T. J.; Vahala, K. J. *Science* **2008**, *321* (5893), 1172−1176.
(2) Favero, I.; Karrai, K. *Nat. Photonics* **2009**, 3 (4), 201−205.
(3) Zalalutdinov, M.; Zehnder, A.; Olkhovets, A.; Turner, S.; Sekaric, L.; Ilic, B.; Czaplewski, D.; Parpia, J. M.; Craighead, H. G. *Appl. Phys. Lett.* **2001**, *79* (5), 695−697.
(4) Metzger, C. H.; Karrai, K. *Nature* **2004**, *432* (7020), 1002−1005.
(5) Arcizet, O.; Cohadon, P. F.; Briant, T.; Pinard, M.; Heidmann, A. *Nature* **2006**, *444* (7115), 71−74.
(6) Gigan, S.; Bohm, H. R.; Paternostro, M.; Blaser, F.; Langer, G.; Hertzberg, J. B.; Schwab, K. C.; Bauerle, D.; Aspelmeyer, M.; Zeilinger, A. *Nature* **2006**, *444* (7115), 67−70.
(7) Schliesser, A.; Del'Haye, P.; Nooshi, N.; Vahala, K. J.; Kippenberg, T. J. *Phys. Rev. Lett.* **2006**, *97* (24), 243905.
(8) Thompson, J. D.; Zwickl, B. M.; Jayich, A. M.; Marquardt, F.; Girvin, S. M.; Harris, J. G. E. *Nature* **2008**, *452* (7183), 72−76.
(9) Anetsberger, G.; Arcizet, O.; Unterreithmeier, Q. P.; Riviere, R.; Schliesser, A.; Weig, E. M.; Kotthaus, J. P.; Kippenberg, T. J. *Nat. Phys.* **2009**, *5* (12), 909−914.
(10) Arcizet, O.; Briant, T.; Heidmann, A.; Pinard, M. *Phys. Rev. A* **2006**, *73* (3), 71−74.
(11) Bagheri, M.; Poot, M.; Li, M.; Pernice, W. P. H.; Tang, H. X. *Nat. Nanotechnol.* **2011**, *6* (11), 726−732.
(12) Hossein-Zadeh, M.; Vahala, K. J. *IEEE Photonics Technol. Lett.* **2008**, *20* (1−4), 234−236.
(13) Wiederhecker, G. S.; Chen, L.; Gondarenko, A.; Lipson, M. *Nature* **2009**, *462* (7273), 633−636.
(14) Chan, J.; Alegre, T. P. M.; Safavi-Naeini, A. H.; Hill, J. T.; Krause, A.; Groblacher, S.; Aspelmeyer, M.; Painter, O. *Nature* **2011**, *478* (7367), 89−92.
(15) Bunch, J. S.; van der Zande, A. M.; Verbridge, S. S.; Frank, I. W.; Tanenbaum, D. M.; Parpia, J. M.; Craighead, H. G.; McEuen, P. L. *Science* **2007**, *315* (5811), 490−493.
(16) Barton, R. A.; Parpia, J.; Craighead, H. G. *J. Vac. Sci. Technol., B* **2011**, *29* (5), 050801.
(17) Chen, C. Y.; Rosenblatt, S.; Bolotin, K. I.; Kalb, W.; Kim, P.; Kymissis, I.; Stormer, H. L.; Heinz, T. F.; Hone, J. *Nat. Nanotechnol.* **2009**, *4* (12), 861−867.
(18) Singh, V.; Sengupta, S.; Solanki, H. S.; Dhall, R.; Allain, A.; Dhara, S.; Pant, P.; Deshmukh, M. M. *Nanotechnology* 2010, *21*, (16).
(19) van der Zande, A. M.; Barton, R. A.; Alden, J. S.; Ruiz-Vargas, C. S.; Whitney, W. S.; Pham, P. H. Q.; Park, J.; Parpia, J. M.; Craighead, H. G.; McEuen, P. L. *Nano Lett.* **2010**, *10* (12), 4869−4873.
(20) Lee, C.; Wei, X. D.; Kysar, J. W.; Hone, J. *Science* **2008**, *321* (5887), 385−388.
(21) Song, X. F.; Oksanen, M.; Sillanpaa, M. A.; Craighead, H. G.; Parpia, J. M.; Hakonen, P. J. *Nano Lett.* **2012**, *12* (1), 198−202.
(22) Barton, R. A.; Ilic, B.; van der Zande, A. M.; Whitney, W. S.; McEuen, P. L.; Parpia, J. M.; Craighead, H. G. *Nano Lett.* **2011**, *11* (3), 1232−1236.
(23) Eichler, A.; Moser, J.; Chaste, J.; Zdrojek, M.; Wilson-Rae, I.; Bachtold, A. *Nat. Nanotechnol.* **2011**, *6* (6), 339−342.
(24) Nair, R. R.; Blake, P.; Grigorenko, A. N.; Novoselov, K. S.; Booth, T. J.; Stauber, T.; Peres, N. M. R.; Geim, A. K. *Science* **2008**, *320* (5881), 1308−1308.
(25) Gabor, N. M.; Song, J. C. W.; Ma, Q.; Nair, N. L.; Taychatanapat, T.; Watanabe, K.; Taniguchi, T.; Levitov, L. S.; Jarillo-Herrero, P. *Science* **2011**, *334* (6056), 648−652.
(26) Yan, J.; Kim, M.-H.; Elle, J. A.; Sushkov, A. B.; Jenkins, G. S.; Milchberg, H. M.; Fuhrer, M. S.; Drew, H. D. *Nat. Nano.* **2012**, *7*, 472−478.
(27) Poot, M.; van der Zant, H. S. J. *Phys. Rep.* **2012**, *511* (5), 273−335.
(28) Teufel, J. D.; Donner, T.; Li, D. L.; Harlow, J. W.; Allman, M. S.; Cicak, K.; Sirois, A. J.; Whittaker, J. D.; Lehnert, K. W.; Simmonds, R. W. *Nature* **2011**, *475* (7356), 359−363.
(29) O'Connell, A. D.; Hofheinz, M.; Ansmann, M.; Bialczak, R. C.; Lenander, M.; Lucero, E.; Neeley, M.; Sank, D.; Wang, H.; Weides, M.; Wenner, J.; Martinis, J. M.; Cleland, A. N. *Nature* **2010**, *464* (7289), 697−703.
(30) Sun, X.; Zheng, J.; Poot, M.; Wong, C. W.; Tang, H. X. *Nano Lett.* **2012**, *12* (5), 2299−2305.
(31) Perahia, R.; Cohen, J. D.; Meenehan, S.; Alegre, T. P. M.; Painter, O. *Appl. Phys. Lett.* **2010**, *97* (19), 191112.
(32) Holscher, H.; Milde, P.; Zerweck, U.; Eng, L. M.; Hoffmann, R. *Appl. Phys. Lett.* **2009**, *94* (22), 223514.
(33) Usami, K.; Naesby, A.; Bagci, T.; Nielsen, B. M.; Liu, J.; Stobbe, S.; Lodahl, P.; Polzik, E. S. *Nat. Phys.* **2012**, *8* (2), 168−172.
(34) Carr, D. W.; Craighead, H. G. *J. Vac. Sci. Technol. B* **1997**, *15* (6), 2760−2763.
(35) Metzger, C.; Favero, I.; Ortlieb, A.; Karrai, K. *Phys. Rev. B* **2008**, *78* (3), 035309.
(36) Kippenberg, T. J.; Rokhsari, H.; Carmon, T.; Scherer, A.; Vahala, K. J. *Phys. Rev. Lett.* **2005**, *95* (3), 033901.

(37) Zalalutdinov, M.; Aubin, K. L.; Pandey, M.; Zehnder, A. T.; Rand, R. H.; Craighead, H. G.; Parpia, J. M.; Houston, B. H. *Appl. Phys. Lett.* **2003**, *83* (16), 3281−3283.

(38) Gysin, U.; Rast, S.; Ruff, P.; Meyer, E.; Lee, D. W.; Vettiger, P.; Gerber, C. *Phys. Rev. B* **2004**, *69* (4), 045403.

(39) Vogel, M.; Mooser, C.; Karrai, K.; Warburton, R. J. *Appl. Phys. Lett.* **2003**, *83* (7), 1337−1339.

(40) Restrepo, J.; Gabelli, J.; Ciuti, C.; Favero, I. *C. R. Phys.* **2011**, *12* (9−10), 860−870.

(41) De Liberato, S.; Lambert, N.; Nori, F. *Phys. Rev. A* **2011**, *83* (3), 033809.

(42) Balandin, A. A.; Ghosh, S.; Bao, W. Z.; Calizo, I.; Teweldebrhan, D.; Miao, F.; Lau, C. N. *Nano Lett.* **2008**, *8* (3), 902−907.

(43) Camerer, S.; Korppi, M.; Jockel, A.; Hunger, D.; Hansch, T. W.; Treutlein, P. *Phys. Rev. Lett.* **2011**, *107* (22), 223001.

dx.doi.org/10.1021/nl302036x | *Nano Lett.* 2012, 12, 4681−4686